Ocean Ambient Noise Studies for Improved Sonar Processing

Martin Siderius and John Gebbie
Portland State University
Electrical and Computer Engineering Department
1900 SW 4th Ave.
Portland, OR 97201
Phone:(503) 725-3223 fax:(503) 725-3807 Email: siderius@pdx.edu

Award Number: N00014-12-1-02050
http://www.ece.pdx.edu/Faculty/Siderius.php

LONG-TERM GOALS

The purpose of this research is to investigate multipath arrival structures that are present in received passive sonar data and exploit this for enhanced passive sonar detection and tracking capability.

OBJECTIVES

Inherent in passive sonar systems are several challenges that any effective system implementation must address. One of these challenges is how to best treat multipath arrivals. In some cases these can be a hindrance while in this research they are exploited. In certain environments, multipath arrivals retain significant coherence with respect to each other. This fact has been noted and exploited in recent decades with the development of the class of techniques known as matched field processing (MFP). While there has been a significant amount of academic focus on developing this approach in the context of the more established array processing methodologies, its practical adoption has been hampered due to the need for accurate environmental models. Despite this shortfall, the conceptual basis of using multipath arrivals to enhance target localization still holds promise. In this project, the emphasis is on analytically and experimentally determining techniques to measure and utilize multipath.

Recent studies into localization of marine mammals have shown that with only rough environmental models, 3-D localization is possible using a single hydrophone [Tiemann, 2006]. The principle of using multipath for range-depth localization is not new, however until recently the computational complexity of applying this to azimuth-dependent bathymetry has been prohibitive. Whale clicks are impulsive, so multipath structure is evident in raw time-domain data. However, this is not true of vessel noise, so this localization concept is extended to pulse compressed time-series data [See publication #1].

Recent advances in robotics, low power embedded computing, and sensor technologies (to name a few) have led to the advent of autonomous underwater vehicles (AUVs). Determining the best ways of designing passive sonar systems for these mobile platforms is an active area of research. In the GLASS'12 experiment performed by CMRE (with Portland State University collaborating), a hybrid (glider/propeller) AUV was outfitted with a compact nose-mounted hydrophone array consisting of tetrahedral and vertical line sub arrays. The small aperture, rigid frame, and high sample rate are

Report Documentation Page

Form Approved
OMB No. 0704-0188

1. REPORT DATE **30 SEP 2013**	2. REPORT TYPE	3. DATES COVERED **00-00-2013 to 00-00-2013**

4. TITLE AND SUBTITLE **Ocean Ambient Noise Studies for Improved Sonar Processing**	5a. CONTRACT NUMBER
	5b. GRANT NUMBER
	5c. PROGRAM ELEMENT NUMBER
6. AUTHOR(S)	5d. PROJECT NUMBER
	5e. TASK NUMBER
	5f. WORK UNIT NUMBER
7. PERFORMING ORGANIZATION NAME(S) AND ADDRESS(ES) **Portland State University,Department of Electrical and Computer Engineering,1900 SW Fourth Avenue,Portland,OR,97207**	8. PERFORMING ORGANIZATION REPORT NUMBER
9. SPONSORING/MONITORING AGENCY NAME(S) AND ADDRESS(ES)	10. SPONSOR/MONITOR’S ACRONYM(S)
	11. SPONSOR/MONITOR’S REPORT NUMBER(S)

12. DISTRIBUTION/AVAILABILITY STATEMENT
Approved for public release; distribution unlimited

13. SUPPLEMENTARY NOTES

14. ABSTRACT

15. SUBJECT TERMS

16. SECURITY CLASSIFICATION OF:			17. LIMITATION OF ABSTRACT	18. NUMBER OF PAGES	19a. NAME OF RESPONSIBLE PERSON
a. REPORT **unclassified**	b. ABSTRACT **unclassified**	c. THIS PAGE **unclassified**	**Same as Report (SAR)**	**11**	

Standard Form 298 (Rev. 8-98)
Prescribed by ANSI Std Z39-18

ideally suited for analyzing multipath. In this work, the underlying concepts of the passive fathometer [Siderius, 2010] are extended to cross-correlate beams steered at multipath arrivals from a passing boat (source of noise) providing for an estimate of azimuth, elevation, and lag between multipath [See publications #2 and #3]. Naturally, this can be used to estimate target position, however the problem can also be turned around to potentially use boat noise as a source of opportunity for estimating geoacoustic properties and the sound speed profile.

APPROACH

This research has taken the multifaceted approach of analyzing multipath with two hydrophones of a bottom-mounted HLA [Publication #1]. Using a very different array configuration consisting of a compact volumetric array [Publications #2 and #3], a different processing modality is adopted which is a fusion of adaptive beam forming and cross-correlation.

WORK COMPLETED

A study on two-hydrophone multipath localization method for small boats has been published [Publication #1]. Two conference proceedings have been generated on the cross-beam correlation technique [Publications #2 and #3]. These were presented at the ICA 2013 in Montreal, and the UAC in Corfu, respectively. A journal article on this topic has been submitted to the Journal of the Acoustical Society of America [Publication #4].

RESULTS

TWO-HYDROPHONE TARGET LOCALIZATION

This work presents a model-based localization technique that leverages reflections from a varying-bathymetry environment to refine estimates of the range and bearing to a small boat using two hydrophones. This work experimentally demonstrates that in an environment that produces multipath, the arrival information available at just two hydrophones encodes sufficient information to provide reasonable estimates of the range of a small boat. Further, varying bathyemtry can be opportunistically utilized to refine bearing.

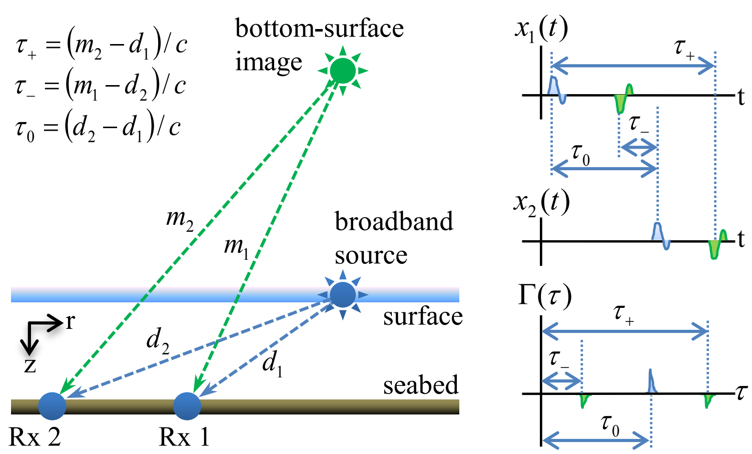

Figure 1: Manifestation of TDOA (τ_0) and ($\tau_\pm$) for the first multipath arrival in a cross-correlation time series.

The geometry of this problem is illustrated in Figure 1 and shows two bottom-mounted hydrophones and a broadband target on the surface. The bottom-surface reflection appears as an image source located two water depths above the surface. The top two diagrammatic plots in Figure 1 show the received time series, $x_1(t)$ and $x_2(t)$. The bottom plot shows the cross-correlation, $\Gamma(\tau)$. The source waveforms, $x_1(t)$ and $x_2(t)$ are represented as a single pulse for illustration purposes, but for a small boat target, they actually consist of continuous broadband noise. However, this does not affect the presence of pulses in $\Gamma(\tau)$ because the noise is pulse compressed through the cross-correlation operation.

Because receiver 2 is farther from the source than receiver 1, both peaks in $x_2(t)$ are shifted later in time to account for the additional travel time. The term τ_0 denotes the time difference of arrival TDOA, and $\tau_\pm$ are the time difference of multipath arrivals, TDOMA. In $\Gamma(\tau)$, the strongest peak is in the center, with an absolute offset at τ_0. The flanking (TDOMA) peaks are produced by the direct arrival from one hydrophone correlating with the multipath arrival from the other hydrophone. As the target initially moves into the far field of the hydrophone pair, τ_- and τ_+ start to converge but are sufficiently large that the flanking peaks are distinct from the TDOA peak, but this separation eventually vanishes in the distant far field. Bathymetric variations affect $\tau_\pm$ because the eigenray path length depends on the depth of each bottom reflection, and this allows for bearing disambiguation.

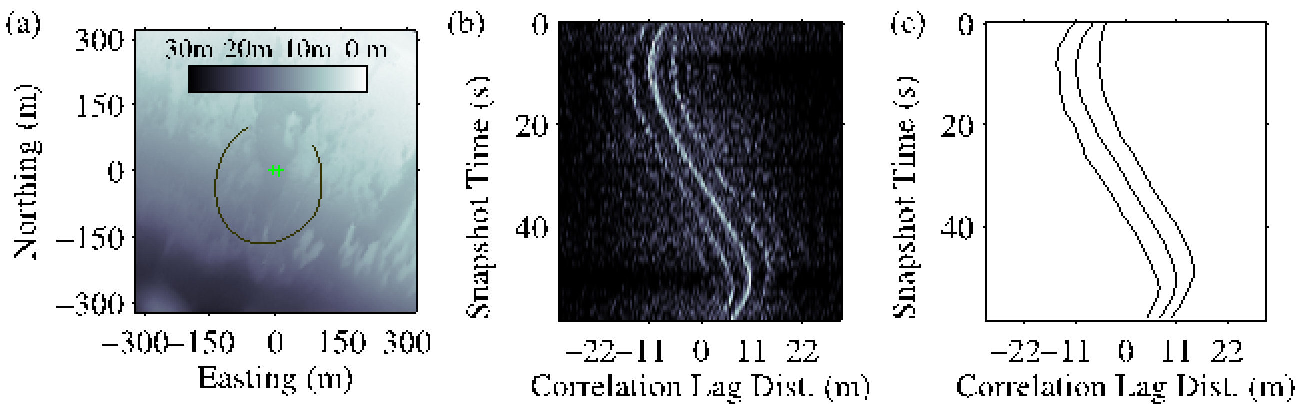

Figure 2: (a) Bathymetry and GPS boat track. The solid line shows the track of the small boat with a counter-clockwise trajectory. The ``+" annotations indicate array element locations. (b) Correlogram showing $10\log_{10}|\Gamma(\tau)|^2$ evolving over snapshot time, plotted using 30 dB of dynamic range and with τ converted to distance. (c) Striation lines for the TDOA (τ_0) and TDOMA ($\tau_\pm$), determined manually. These values facilitate de-noising the correlogram, in which they serve as the parameters to $\hat{\Gamma}(\tau)$ defined in Eq. 1.

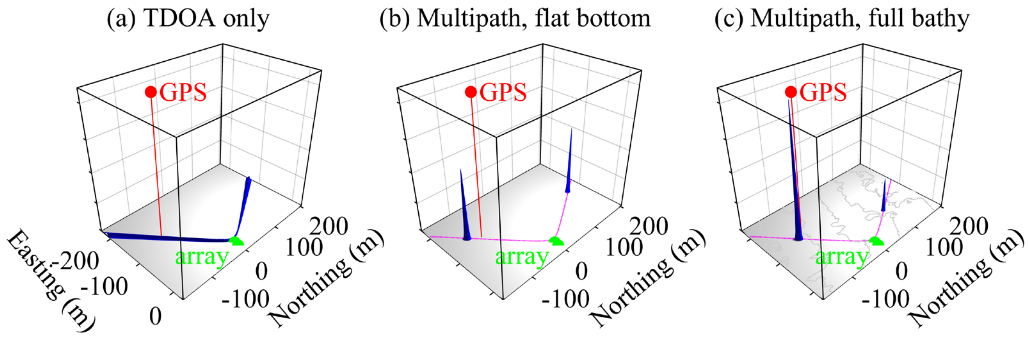

Figure 3: (a) Comparison of ambiguity surfaces, $\Phi(\mathbf{x})$, for a single snapshot showing the effect of utilizing multipath and bathymetry information. Plots are normalized to unit volume to show the relative concentration of target location certainty. (a) A hyperbolic ambiguity is associated with only using the TDOA (first) term of Eq. 2. (b) Inclusion of multipath [the latter two terms of Eq. 2 and the assumption of a flat seabed cause the hyperbola to collapse to a single range, but a left-right ambiguity remains. (c) Using actual bathymetry to determine the position of the bottom-surface image moves the range estimate on the near side closer to the GPS measurement and allocates a greater amount of target location certainty to it than the ambiguous peak. Contour lines are shown at 2.5 m intervals. For (b) and (c), the hyperbola defined by the TDOA, τ_0, is also shown.

A correlogram is shown in Figure 3(b) in which multipath effects are evident. The strong, center striation is the correlation of direct arrivals. This is supported by the fact that as the target circles around the array, this striation stays between ±11 m, which are the limits for the correlation lag distance for the configured hydrophone spacing of 11 m. The multipath-with-direct correlations are visible as ``shadow" striations that run adjacent to the main striation. All these striation lines were manually traced using MATLAB and are shown in Figure 2(c). Shadow striations from higher-order eigenrays are also faintly visible throughout the entire run.

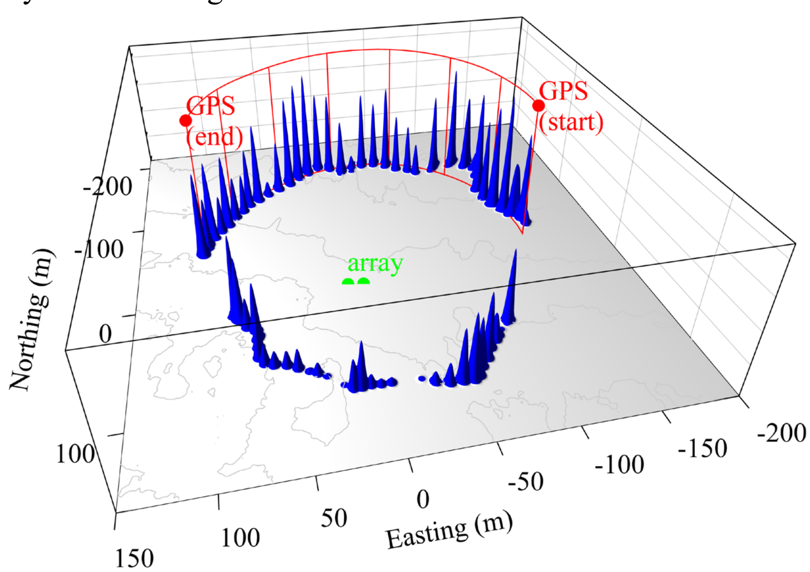

Figure 4: Ambiguity surfaces, $\Phi(\mathbf{x})$, for the sequence of snapshots between 13.5 and 47.5 s from the track shown in Figure 3(a)-Figure 3(c). This period corresponds to when the boat is to the south of the array and sweeping through bearing angles from end-fire to end-fire. The camera is pointed mainly southward. The peaks on the far side of the array (where the boat is located) track well with the GPS data and have a higher certainty score than the peaks on the near side.

A comparison of localization using only TDOA [corresponding to using just the first term of Eq. 2] with both TDOA and TDOMA [all terms of Eq. 2] is shown in subplots (a) and (b) of Figure 3. The effects of using a flat seabed versus actual bathymetry are shown in subplots (b) and (c). The full ambiguity function, $\Phi(\mathrm{x})$, is shown for several snapshots throughout the boat track in Figure 4. The image data in Figure 3 and Figure 4 were post-processed with a 2-D Hann filter to aid visualization of narrow features.

This works presents a technique for localizing a small boat using multipath arrivals recorded on two bottom-mounted hydrophones. The correlations necessary to perform this inversion come from the lowest-order eigenrays, which are shown to be relatively stable features in a correlogram. Range information can be extracted from these features using image positions to estimate path length differences between direct and multipath eigenrays. Use of a bathymetry database for multipath ray calculation improves range localization and diminishes the left-right ambiguity typically associated with line arrays, but this is only possible in the presence of bathymetric variations. This experiment shows localization out to roughly 14 water depths, which would correspond to a much longer range in deeper water. Experimental results from passive acoustic measurements of a small boat maneuvering in a shallow-water harbor environment were validated by comparison with the boat's GPS log.

CROSS-BEAM CORRELATION USING A COMPACT VOLUMETRIC ARRAY FOR MEASURING MULTIPATH

A technique is presented for simultaneously measuring the elevation angle and time lag between multipath arrivals by cross-correlating beams from a noise source using a compact volumetric array. This is an extension of the adaptive passive fathometer [Siderius *et al.*, J. Acoust. Soc. Am. 127, 2193-2200 (2010)] but is applied to boat noise in very shallow water. Experimental results are presented from GLASS'12 which employed a hybrid autonomous underwater vehicle outfitted with a compact volumetric nose array as a data collection platform. Ray tracing is employed to interpret the multipath arrival structure as the boat passes by the array. A multi-target scenario is synthesized by adding together two boat passes showing that adaptive cross-beam correlation operates well in the presence of interference. This technique is then discussed in the context of different application areas, such as sensitivity to the water sound speed profile, target localization, and geoacoustic inversion.

It has been shown that cross-correlating the end-fire beams of a vertical line array suspended in an ambient noise field can produce a reflectivity profile of the seabed. This “passive fathometer” technique was first demonstrated by [Siderius 2006]. It works by pulse compressing downward-traveling broadband surface noise with the upward-traveling reflection of that same noise waveform from the seabed. The resulting “pulse” shows up in a time-series plot at an offset that corresponds to the time it takes for the noise signal to travel from the array, to the seabed, and back.

a)  b) 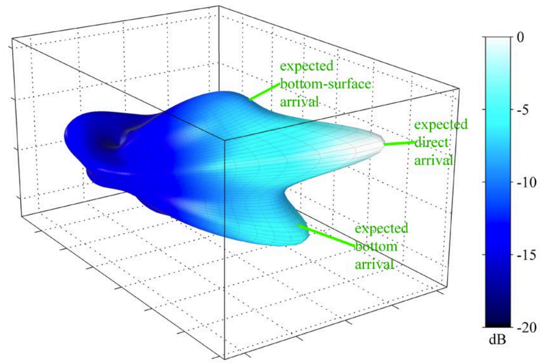

Figure 5: (a) Tetrahedral and line array mounted to the nose of the eFolaga AUV. Five elements comprise a vertical line array. The middle element of the line is one vertex of a tetrahedron. (b) Adaptive beamformer output shown in a 3-D coordinate space local to the array. Computed at 7 kHz with a 1 kHz bin width. The line annotations indicate the direction of arrival for the first multipath eigenrays. Axes are scaled equally.

This section describes an extension of the adaptive passive fathometer and presents a new technique for measuring multipath called cross-beam correlation. It has some important differences with the passive fathometer, in that opportunistic source signals originate from a boat instead of from noise directly overhead from breaking waves. Also, the array is compact and volumetric, shown in Figure 5(a), so operates at higher frequencies. This technique allows individual multipath arrivals to be isolated in elevation angle using short snapshot averaging to break the multipath coherence. Long snapshot cross-beam correlation is then used to measure the time-lag of multipath arrivals, which is applied in the same way as the passive fathometer. This is verified experimentally with a small boat as a noise source. A multi-target scenario is synthesized by adding together two separate boat passes showing adaptive rejection of off-bearing interference.

This is a new measurement scheme using noise sources of opportunity. Multipath has been measured using a variety of other methods, but an advantage of using a compact array is it can be mounted on a mobile platform, such as an AUV. Combined with being able to leverage noise present in the environment for remote sensing, this has many practical uses.

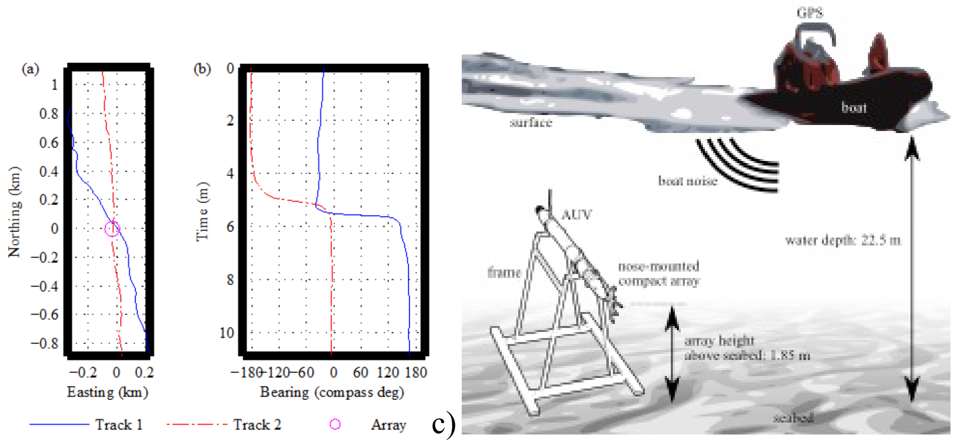

Figure 6: (a) Tracks of the same boat for two passes by the array, taken from GPS records. (b) Compass bearings of the two same two tracks. A multi-target scenario is simulated by adding the acoustic data from each track. This plot shows how they are aligned in time. (c) Exerimental Setup

Despite suffering technical problems with the ballasting subsystem, acoustic data recordings were collected by mounting the AUV on a rigid frame, as illustrated in Figure 6(a). A small rubber boat with an outboard engine outfitted with a portable GPS data recorder maneuvered in the vicinity of the array. The speed of the boat was roughly 3 m/s for both tracks. Selected portions of the track of the boat are shown in Figure 7(a). Besides the R/V *Alliance*, there were few vessels detected in the local region. To simulate a multiple target scenario in which the positions of each vessel are known, acoustic data from two times when the boat passed the array were added together. The time alignment of these two passes, showing the relative bearings of each pass are shown in Figure 6(b).

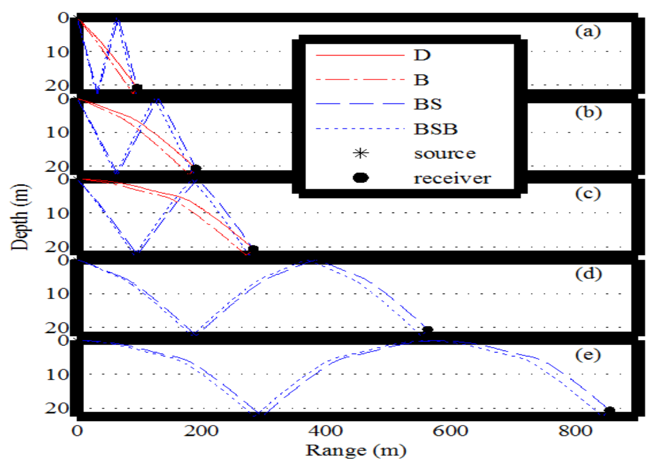

Figure 7: Ray trace using Bellhop. Only D, B, BS, and BSB eigenrays are shown. Note the culling of the D and B eigenrays as the range approaches 300 m. Panel (c) represents the maximum range of the D eigenray, which corresponds to a 0 degree ray launch angle. Likewise, panel (e) shows the maximum range of the BS eigenray.

Figure 7 shows a set of eigenrays computed with Bellhop. The paths of these rays can be understood by noting the site has a negative gradient in the sound speed profile (i.e. the trend shows decreasing sound speed with increasing depth). This causes rays to bend toward the seabed; an effect that is amplified as rays are launched closer to the horizontal. Note that Figure 7(c) is the last panel that

shows a direct (D) and bottom-bound (B) eigenray. This corresponds to the maximum range for which the D eigenray exists. The launch angle for the D eigenray at that range is zero, meaning that just beyond that range the ray must first reflect off the seabed to be received by the array, which essentially kills off the D eigenray. The same phenomenon happens for the bottom-surface (BS) ray; its limiting range is shown in Figure 7(e).

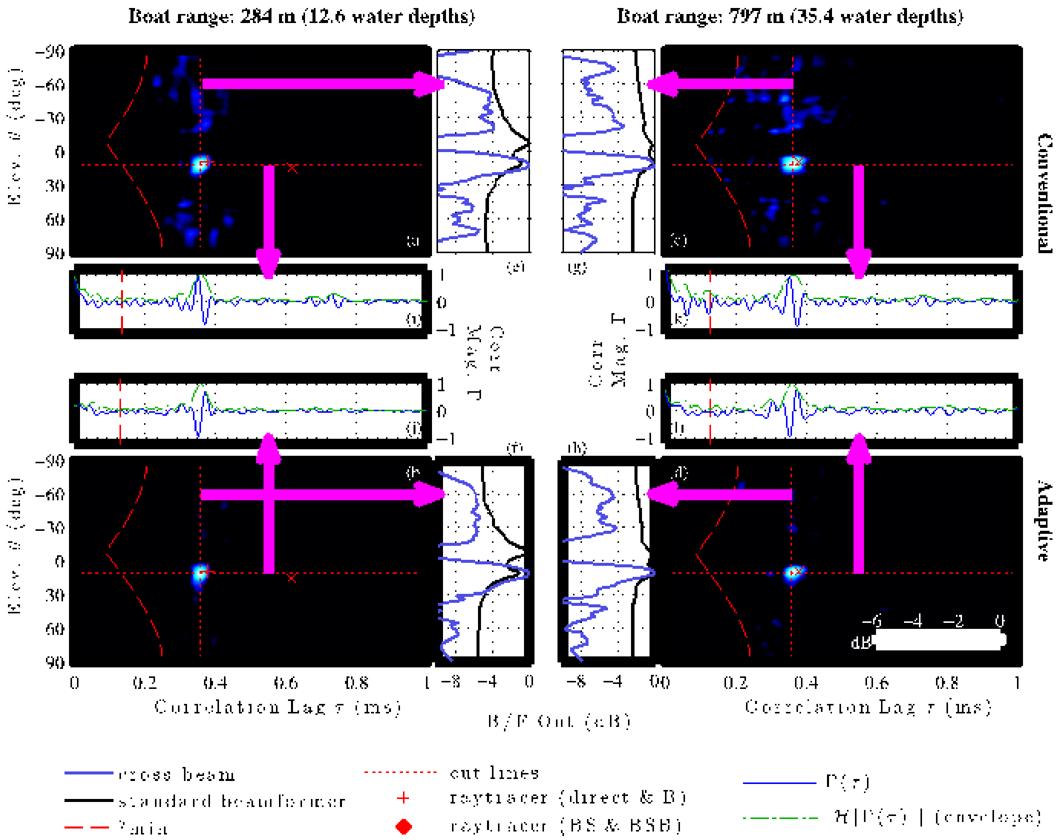

Figure 8: Cross-beam correlation of the strongest arrival with other elevation angles along the same azimuthal direction at two boat ranges in Track 1. (a-d) Correlation power envelope at each elevation angle and time lag. (e-h) A vertical slice of the cross-beamformer taken at the measured multipath lag compared with short-snapshot standard beamformer output. (i-l) Cross-beamformer time series output at the measured multipath elevation angle showing the actual waveform and its envelope.

The left and right halves of Figure 8 show the boat at different ranges, and the top and bottom halves compare conventional with adaptive beamforming. For the closer boat range (left half), the SSP supports D and B eigenrays, whereas in the more distant boat range (right half) these have gone away leaving the BS and BSB eigenrays as the strongest arrivals. In each instance, a peak appears close to the ray tracer predictions in space and time. For the closer range, the BS with BSB correlation is not visible since the array is being steered at the D eigenray arrival instead of the BS arrival. While it is possible the beam corresponding to the BS eigenray arrival is close enough to the D beam to allow for leakage, greater losses in both of the higher-order eigenrays reduce the relative power of their correlation. Slices through the elevation angles at the detected peak are compared with the standard beamformer in Figure 8(e-h). Correspondence between the arrival angle of the lower peak from the standard beamformer and the cross-beam output indicate that the lower peak is, in fact, a coherent

multipath arrival. The significance of this is being able to identify that two peaks in the standard beamformer output are mutually coherent at a specific time lag offset. This is not information that is available from a standard beamformer output. The cross-beam correlation time series for the strongest correlation is shown in Figure 8(i-l).

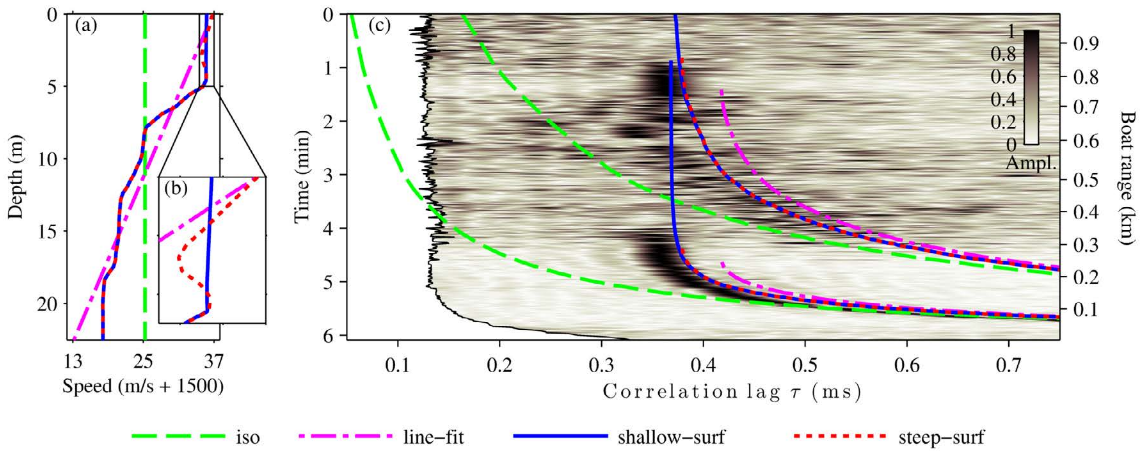

Figure 9: (a-b) Different SSPs used to configure the ray tracer. (c) Correlogram with overlays showing the multipath lags resulting from each SSP. There are two lines for each SSP which correspond to the lags between each of the two sets of eigenray pairs (D-with-B and BS-with-BSB). Note the ranges at which rays are culled match well with the CTD SSP whereas when the near surface part of the SSP is changed to be isovelocity, this range changes dramatically.

The multipath lag of cross-beam correlation is highly sensitive to the SSP. Initially in this study, an isovelocity model was adopted. This produced accurate predictions of the multipath lag out to about 100 m, but beyond that lag predictions were smaller than observed. These observations became explainable once a ray model was used and configured with the measured SSP. The downward refracting profile causes an increase in the lag, and its effect starts to become more pronounced at about 100 m range. This is evident by comparing the multipath lags computed using different SSPs to the acoustic data in Figure 9. The isovelocity model clearly diverges from the acoustic data around this range whereas the other SSPs, which are downward-refracting, produce measurable lags out to farther ranges. The downward refraction causes rays launched near the surface to have steeper angles as they pass through the array depth. This implies that there is a minimum bound on the lag between a downward-traveling ray received at the array and the subsequent ray that bounces off the seabed. This appears at roughly 0.36 ms.

A cross-beam correlation technique has been presented showing that cross-correlating beams steered at multipath arrivals provides information about the received elevation angle and relative time lag. The compact size of the array minimized the white noise correlation artifact allowing multipath to be measured. The rigid frame on which the elements were mounted enabled the use of an aggressively-tuned MPDR adaptive beamformer for rejection of off-bearing interference. Adaptive nulling of multipath arrivals was also demonstrated using short snapshots that are insensitive to coherence between rays.

IMPACT/APPLICATIONS

This work may facilitate more effective passive sonar detection techniques in environments that support strong multipath. It is particularly effective for broadband targets, but aspects of it may also be applicable to narrowband targets. There is a need for such algorithms that are robust to reasonable amounts of environmental mismatch. As a passive method, it can be designed into a system used for covert activities, low power applications and can be used even in environmentally restricted areas. Opportunistic sources have a significant amount of practical utility. In this experimental design, multipath arrivals from the small boat were detected out to about 35 water depths, which corresponded to a little over 800 meters in the shallow waters of the experimental site. The downward-refracting SSP was the limiting factor in this the GLASS'12 dataset causing culling of rays at specific distances, which was another piece of information clearly evident in the data. Moored passive equipment can be cumbersome to deploy and communicate with, and AUV-mounted devices are an attractive alternative. The AUV used in GLASS'12 is designed to operate in both glider and propeller-driven modes giving it many possibilities for collecting non-acoustic environmental data. The technique presented in Publication #4 could potentially facilitate on-board data fusion for analysis of both nearby targets and environment in an entirely passive manner. Beyond remote monitoring, multi-target localization and range estimation could help provide collision avoidance capabilities to on-board control software.

REFERENCES

[Aubauer 2000] R. Aubauer, M. O. Lammers, and W. W. L. Au, "One-hydrophone method of estimating distance and depth of phonating dolphins in shallow water," *The Journal of the Acoustical Society of America*, vol. 107, no. 5, pp. 2744-2749, May 2000.

[Blanc-Benon 1995] P. Blanc-Benon, "Implication of shallow waters for source localization: Time-delays estimation versus matched-field processing," in*OCEANS '95. MTS/IEEE. Challenges of Our Changing Global Environment. Conference Proceedings.*, vol. 2. IEEE, Oct. 1995, pp. 826-831 vol.2.

[Bruno 2010] M. Bruno, K. W. Chung, H. Salloum, A. Sedunov, N. Sedunov, A. Sutin, H. Graber, and P. Mallas, "Concurrent use of satellite imaging and passive acoustics for maritime domain awareness," in *International Waterside Security Conference (WSS), 2010*. IEEE, Nov. 2010, pp. 1-8.

[Carter 1973] G. C. Carter, A. H. Nuttall, and P. G. Cable, "The smoothed coherence transform, " *Proceedings of the IEEE*, vol. 61, no. 10, pp. 1497-1498, Oct. 1973.

[Gebbie 2012] J. Gebbie, M. Siderius, J. Allen, and G. Pusey, "Small boat localization using time difference of multipath arrivals from two bottom mounted hydrophones," in *European Conference on Underwater Acoustics*, Edinburgh, UK, Jul. 2012.

[Hamilton 1992] M. Hamilton and P. M. Schultheiss, "Passive ranging in multipath dominant environments. i. known multipath parameters," *Signal Processing, IEEE Transactions on*, vol. 40, no. 1, pp. 1-12, Jan. 1992.

[Harrison 2002] C. H. Harrison and D. G. Simons, "Geoacoustic inversion of ambient noise: A simple method," *The Journal of the Acoustical Society of America*, vol. 112, no. 4, pp. 1377-1389, Oct. 2002.

[Harrison 2008] C. H. Harrison, "Target detection and location with ambient noise," *The Journal of the Acoustical Society of America*, vol. 123, no. 4, pp. 1834-1837, Apr. 2008.

[Jensen 2000] F. B. Jensen, W. A. Kuperman, M. B. Porter, and H. Schmidt, *Computational Ocean Acoustics*. New York: Springer-Verlag New York, Inc., 2000.

[Nosal 2006] E. Nosal and L. Neilfrazer, "Track of a sperm whale from delays between direct and surface-reflected clicks," *Applied Acoustics*, vol. 67, no. 11-12, pp. 1187-1201, Nov. 2006.

[Schmidt 1972] R. Schmidt, "A new approach to geometry of range difference location," *Aerospace and Electronic Systems, IEEE Transactions on*, vol. AES-8, no. 6, pp. 821-835, Nov. 1972.

[Siderius 2006] M. Siderius, C. H. Harrison, and M. B. Porter, "A passive fathometer technique for imaging seabed layering using ambient noise," *The Journal of the Acoustical Society of America*, vol. 120, no. 3, pp. 1315-1323, Sep. 2006.

[Siderius 2010] M. Siderius, H. Song, P. Gerstoft, W. S. Hodgkiss, P. Hursky, and C. Harrison, "Adaptive passive fathometer processing," *The Journal of the Acoustical Society of America*, vol. 127, no. 4, pp. 2193-2200, Apr. 2010.

[Tiemann, 2006] C. O. Tiemann, A. M. Thode, J. Straley, V. O'Connell, and K. Folkert, “Three-dimensional localization of sperm whales using a single hydrophone”, J. Acous. Soc. Am. **120**, 2355-2365 (2006).

[Tiemann 2008] C. O. Tiemann, "Three-dimensional single-hydrophone tracking of a sperm whale demonstrated using workshop data from the bahamas," *The Journal of the Canadian Acoustical Association*, vol. 36, no. 1, pp. 67-73, Mar. 2008.

[Van Trees 2002] H. L. Van Trees, *Optimum Array Processing (Detection, Estimation, and Modulation Theory, Part IV)*, 1st ed. John Wiley & Sons, Inc., Mar. 2002.

PUBLICATIONS

1. J. Gebbie, M. Siderius, R. McCargar, J. S. Allen, and G. Pusey, “Localization of a noisy broadband surface target using time differences of multipath arrivals,” The Journal of the Acoustical Society of America Express Letters, vol. 134, no. 1, pp. EL77–EL83, Jun. 2013. [Online]. Available: http://dx.doi.org/10.1121/1.4809771 [accepted, refereed]
2. J. Gebbie, M. Siderius, P. L. Nielsen, J. H. Miller, S. Crocker, and J. Giard, “Small boat localization using adaptive three-dimensional beamforming on a tetrahedral and vertical line array,” in ICA 2013 Montreal. Montreal, Canada: ASA, Jun. 2013, p. 070072. [Online]. Available: http://dx.doi.org/10.1121/1.4800565 [conference]
3. J. Gebbie, M. Siderius, P. L. Nielsen, J. Miller, S. Crocker, and J. Giard, “Small boat localization using adaptive 3-D beamforming on a tetrahedral and vertical line array,” in 1st International Conference & Exhibition on Underwater Acoustics, Corfu, Greece, Jun. 2012, p. 42. [conference]